Int J Adv Manuf Technol (2018) 94:1387–1396
DOI 10.1007/s00170-017-0965-y

ORIGINAL ARTICLE

The Bauschinger effect and mechanical properties of AA5754 aluminum alloy in incremental forming process

Xunzhong Guo [1,2,3] · Yanbo Gu [1,2] · Hui Wang [2,4] · Kai Jin [2,3] · Jie Tao [1,2,3]

Received: 30 March 2017 / Accepted: 14 August 2017 / Published online: 29 August 2017

Abstract This study aims to explore the Bauschinger effect and mechanical properties of 5754 aluminum alloy and their relationship through parts manufactured by incremental forming technology. Pyramidal parts with five different wall angles were formed using incremental forming after which tensile samples from each of the parts were prepared and tested. The experimental results indicated that the Bauschinger effect existed during incremental forming of the aluminum alloy. It was also found that the level of the Bauschinger effect, yield strength, and ultimate tensile strength increased with the expanding wall angle. Compared with the influence of the Bauschinger effect, the work hardening plays a leading role in the change of mechanical properties. Based on the study results, the formulas for predicting the mechanical properties at different wall angles are obtained. Understanding the Bauschinger effect and mechanical properties can help to guide incremental forming simulation and process development of parts manufactured by incremental forming.

✉ Hui Wang
770494571@qq.com

[1] College of Material Science and Technology, Nanjing University of Aeronautics and Astronautics, Nanjing 211100, People's Republic of China

[2] Institute of Advanced Materials and Forming Technology, NUAA, Nanjing 211100, People's Republic of China

[3] Jiangsu Key Laboratory of Nuclear Energy Equipment Materials Engineering, Nanjing 211100, People's Republic of China

[4] College of Mechanical and Electrical Engineering, Nanjing University of Aeronautics and Astronautics, Nanjing 210016, People's Republic of China

Keywords Bauschinger effect · Mechanical properties · Incremental forming · Wall angle

1 Introduction

As a way to efficiently reduce energy usage and decrease pollution, conventional steels are being replaced with aluminum alloys in an increasing number of applications. However, the reduced formability level of various aluminum alloys is a technical hurdle to overcome in many applications. However, incremental forming is an advanced forming technology that can improve the formability of materials [1] and represents one possible solution. Hence, research on the incremental forming of aluminum alloys is of great significance to application of aluminum alloys as well as the use of this forming technology.

The incremental forming process of sheet metal is a new and flexible manufacturing technique. The basic principle of sheet metal incremental forming is based on rapid prototyping, or "layered manufacturing." In the incremental forming process, the tool path is usually divided into several layers across the height direction of the part, and the forming tool completes incremental deformation by moving along the tool path.

During the sheet incremental forming process, a forming tool, a blank holder, a backing plate, and a sheet metal blank are used [2] (shown in Fig.1a). The sheet metal blank is clamped and held in the proper position before the process is initiated, supported by the backing plate. Also, the dimensions of the opening of the backing plate define the working area of the forming tool. Due to the fact that incremental forming uses only simple dies or no dies, the process reduces the time needed for die design and significantly reduces cost [4, 5]. Consequently, it is especially suitable for producing single

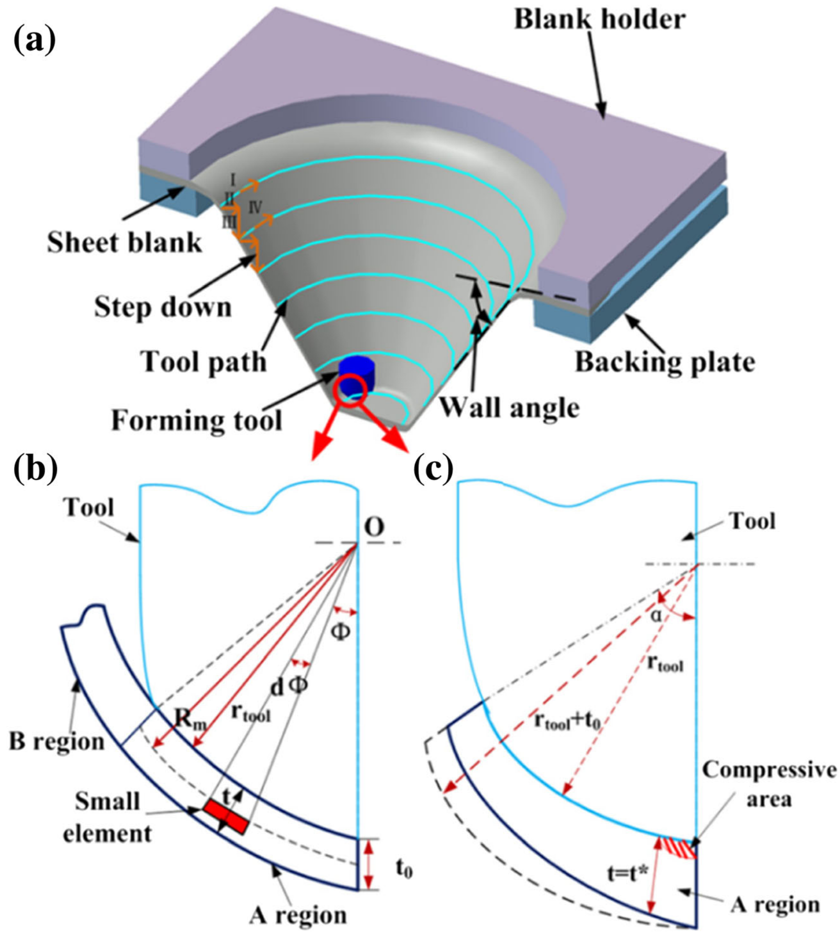

Fig. 1 Schematic representation of the incremental forming process. **a** Overall cross-section view. **b** A detailed cross-section view in spherical co-ordinate [3]. **c** Compressive area [3]

and small batch production parts. In addition, the formability of sheet metal blank in incremental forming tends to be higher than in traditional stamping processes [1]. Furthermore, complicated parts that require thin wall can also be obtained by utilizing incremental forming. Thus, the incremental forming process has begun to play an important role in many fields, such as aerospace engineering, aviation engineering, and automobile prototype manufacturing.

Incremental forming has been widely studied by many researchers. Shrivastava and Tandon studied the effect of grain size on the forming forces in the incremental forming process and discovered that the peak-forming force decreases with an increase in grain size [6]. Shanmuganatan and Kumar presented mathematical models that describe effect of the incremental forming parameters on average thickness and surface roughness of Al3003 aluminum alloy part [7]. Gatea et al. showed that the deformation, strain, and thinning were significantly influenced by the wall angle during the incremental forming process [8]. However, most studies have been focused on the formability limitations and forming mechanism. Few have considered the Bauschinger effect and mechanical properties of the parts manufactured by incremental forming. Hagan studied the effects of wall angles on Al3003 strain hardening of incremental forming parts by means of offsetting the stress-strain curves after forming [9]. However, the existence and conditions of the Bauschinger effect was not revealed. Jin et al. presented a JIS SS400 steel constitutive model which combines a mixed isotropic-kinematic hardening model with the Lematire damage model, and the model can predict the Bauschinger effect and fractures [10]. A comparison of numerical analysis results and data obtained experiments based on cyclic loading validated the model. Jin et al. applied it to a numerical model and found that it can predict the deformation, thickness, shape, and fracture very accurately during incremental forming. However, they only considered the Bauschinger effect in the constitutive model of steel incremental forming. The Bauschinger effect in incremental forming has not been further studied, and the influence of process parameters of incremental forming on the Bauschinger effect remains unknown. However, the Bauschinger effect in incremental forming also depends on the material and the Bauschinger effect has yet to be verified for other types of metals, such as aluminum alloy. Therefore, further studies are needed to investigate the Bauschinger effect in incremental forming. Jun-Chao et al. only took tensile specimens in different zones of a single part to study the mechanical properties of incremental forming [11]. The influence of wall angle on mechanical properties has not been investigated.

AA5754 aluminum alloy, which is an Al–Mg alloy, has properties such as good corrosion resistance, moderate strength and weldability, and the excellent properties have made it more attractive for usage applied in the automotive industry. Meanwhile, incremental forming is also suitable for the research and development of prototype cars. Therefore, it is beneficial to study incremental forming of AA5754 aluminum alloy. In this study, the existence of the Bauschinger effect in incremental forming of AA5754 aluminum alloy is demonstrated. The influence of wall angle on the Bauschinger effect and mechanical properties of parts formed by incremental forming is also investigated using tensile tests performed on specimens taken from the side wall of AA5754 parts manufactured by incremental forming.

Finite element simulation is being applied more and more to the research and production of forming, and the constitutive model has a direct influence on the accuracy and validity of the simulation model. The material models used in conventional forming generally do not consider the Bauschinger effect due to non-cyclic loading. Compared with the simple loading of conventional forming, such as stamping, the loading of incremental forming is very complicated. The loading has an impact on the creation of material models. However, the study of incremental forming takes little account of the effect of complex loading on the material model. Most models of incremental forming are built according to the stamping model. The discovery of the Bauschinger effect in incremental forming of aluminum alloy and the study of the Bauschinger effect provide a more refined constitutive model that can be used to simulate incremental forming of aluminum alloy. For more accurate predictions of strain and stress distribution, fracture prediction, and spring-back, it is essential to establish a suitable constitutive model that contains the Bauschinger effect in incremental forming simulation. Such a model provides important theoretical guidance for building more perfect and correct constitutive model in incremental forming simulation of aluminum alloy. Meanwhile, the mechanical properties of aluminum alloys will change through complex process path in incremental forming. The mechanical properties of the parts after incremental forming were investigated, and the influence of forming angle on mechanical properties was investigated. Through study of mechanical properties, it is possible to understand the load-bearing capacity and application range of incremental forming parts. The study in this paper is of great significance to the further research and practical application of incremental forming technology.

2 Experimental procedure

2.1 Incremental forming experiment and strain measurement

Cold-rolled AA5754-O sheet of 2.0 mm thickness was selected as the work material for the incremental forming experiments. Before the actual forming experiments, a pyramidal shape was designed such that prepared tensile specimens could easily be obtained from the part walls. The bottom dimension of the pyramidal parts was 190.0 mm × 175.0 mm. The initial size of the blank was 230.0 mm × 215.0 mm taking the backing plate and the blank holder into consideration. Prior to forming, strain grids, with 1.0 mm diameter circle and 2.0 mm pitch, were printed on the surface of the AA5754-O sheet blanks using silk screen printing. The sheet blank was then fixed on the working stand with the backing plate and the blank holder. Secondly, the forming tool with 10.4 mm hemispherical end, controlled by a CNC machining center, moved along the trajectory of a G code. In the forming process, the feed rate of the moveable tool without rotation was set at 25.0 mm/s and the step down was 0.2 mm. The surface of the blank was lubricated by oil to reduce friction as much as possible in order to improve the surface quality.

Finally, pyramidal parts having wall angles of 20°, 30°, 40°, 50°, and 60° were fabricated as shown in Fig. 2. The forming depth of the parts with a wall angle of 20° and 30° was 25.0 and 40.0 mm, respectively, while that of the parts with a wall angle of 40°, 50°, or 60° was 60.0 mm. The design of the forming depth is due to the limitations of the forming depth of the parts by the geometric factor and the length of the tensile specimens. A grid strain measurement system, ARGUS, was used to measure the global strain of the pyramidal parts after incremental forming was completed.

2.2 Tensile testing

Tensile specimens were cut from the 2-mm-thick AA5754-O sheet by Wire Electrical Discharge Machining. Three specimens were taken perpendicular to the rolling direction with the size of each specimen being in accordance with the ASTM D638-2003 test standard. Similarly, tensile specimens were cut from the sidewalls of parts formed by incremental forming. All specimens were taken perpendicular to the rolling direction and the tool path, for each wall angle part. Figure 3 shows the layout obtained from the tensile specimens of the parts formed by incremental forming. The dashed arrow demonstrates the rolling direction, and the solid-line arrow indicates the movement direction of the tool. Tensile testing of all specimens was performed with a tensile testing machine with the cross-head travel speed being set at a constant value of 0.017 mm/s.

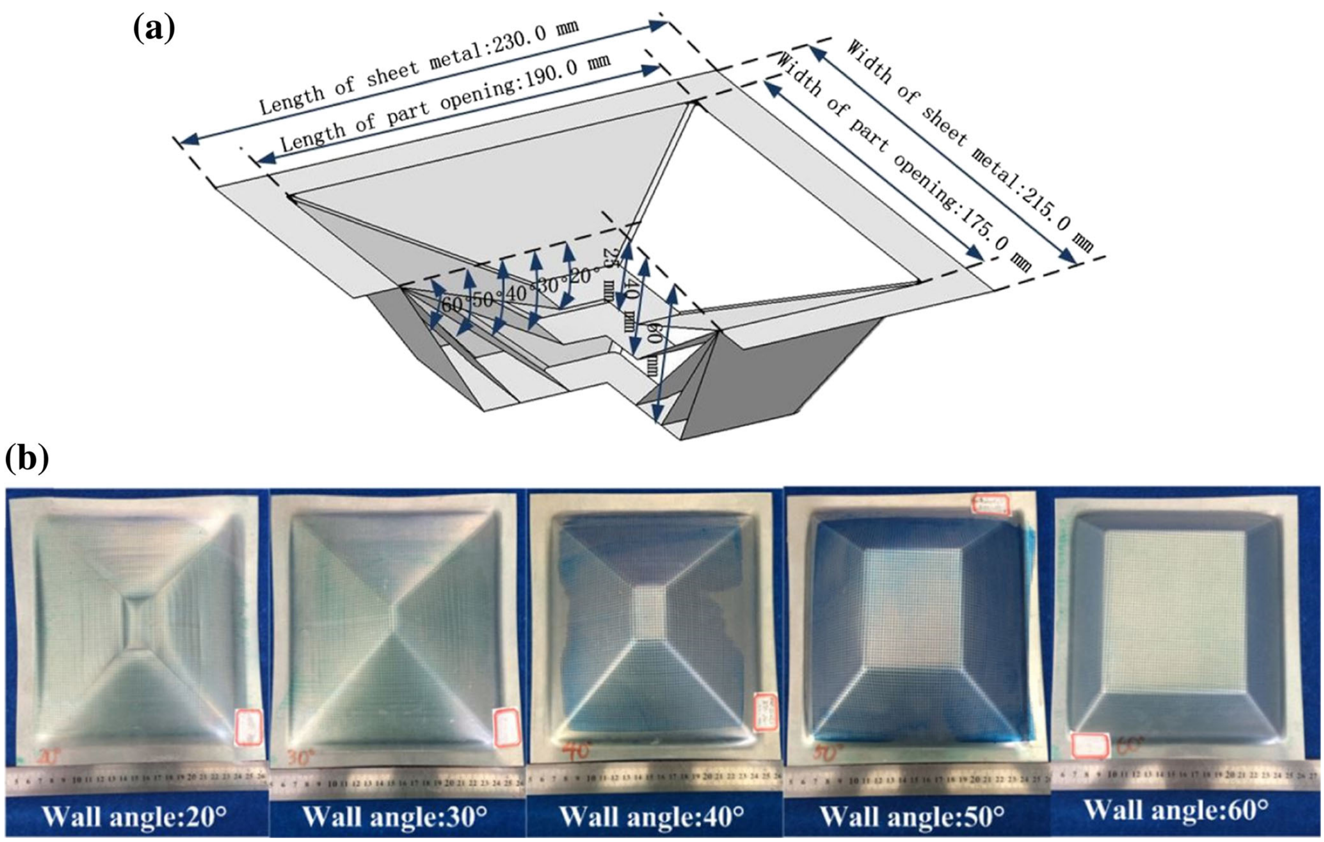

Fig. 2 Incremental forming parts. **a** Schematic representation of each wall angle. **b** Parts formed by incremental forming

3 Results and discussions

3.1 Constitutive equation of AA5754-O

As shown in Fig. 4, the true stress-strain curves of the blank material were obtained by experimental data. It can be observed that the difference among the three true stress-strain curves is insignificant.

In this paper, the fitting curve of three stress-strain curves in Fig. 4 was set as the true stress-strain curve of AA5754-O for the subsequent research, and the yield strength, ultimate tensile strength, and uniform elongation of AA5754-O were 124.0 MPa, 290.0 MPa, and 19.4%, respectively.

A log plot of the plastic region true stress-strain curve in was fitted to a straight line, and it can be observed that the fit between the true stress-strain curve data and the line was very good (Fig. 5). Based on the curve fit, the material was modeled using the Hollomon equation shown in Eq. (1).

$$ln(\sigma) = nln(\varepsilon) + ln(K) \tag{1}$$

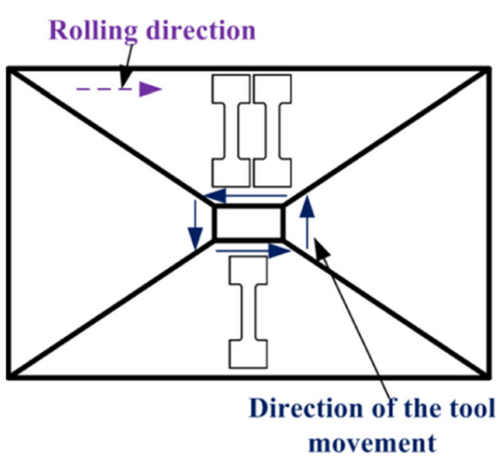

Fig. 3 Layout of tensile specimens cut from parts formed by the incremental forming process

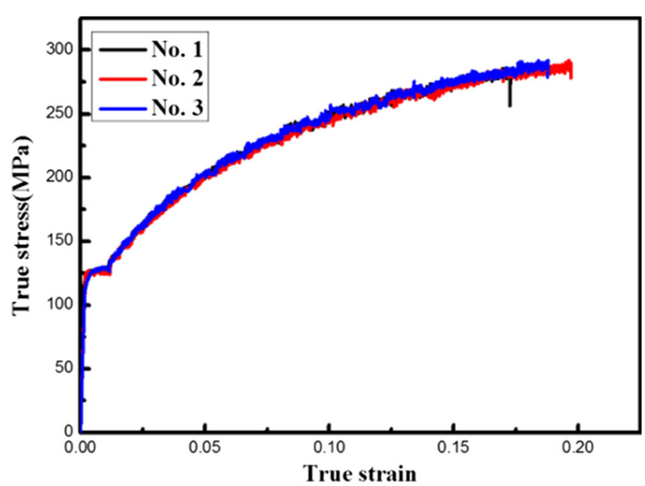

Fig. 4 The true stress-strain curves for AA5754-O

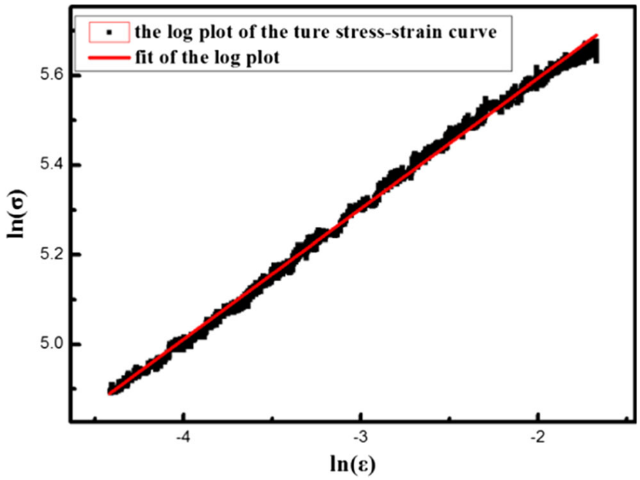

Fig. 5 Fit of the log plot of the true stress-strain curve

where σ is the true stress, n is the strain hardening exponent, ε is the true strain, and K is the strength coefficient. Therefore, the constitutive equation of AA5754-O, which was used to obtain the true stress-strain curve of isotropic work hardening, is expressed in the following equation:

$$\sigma = 481.97\varepsilon^{0.29} \quad (2)$$

3.2 The Bauschinger effect in incremental forming process

A detailed cross-sectional view of incremental forming is presented in Fig. 1b. Region A is the area where the tool contacts the sheet during the incremental forming process. Furthermore, region B is formed, adjacent to region A, and does not get in contact with the tool. Region B is approximately in plane strain state and the tangential strain is considered as zero [3, 12]. The sheet in region A is strained and bent by the tool. Hence, the deformation in region A is a combination of stretching and bending [3, 13, 14]. The middle surface of the sheet can be approximately considered as a neutral surface if the pure bending deformation without any stretching is not excessively high. The original neutral surface offsets to the inner surface, when the stretching is superimposed on the pure bending deformation [3].

The inner surface of the sheet is simultaneously under the compression strain of bending deformation and the tensile strain of stretching deformation [3]. The outer surface of the sheet is simultaneously under the tensile strain of bending deformation and the tensile strain of stretching. The tensile strain of stretching can be represented by the tensile strain at the neutral surface of the sheet, if the bending deformation is not taken into account [3]. Supposing that the deformation is under the plane strain and the tangential strain is zero, the tensile strain due to stretching at the intermediate surface can be calculated by Eq. (3) [3]:

$$\varepsilon_{\text{stretching}} = -\varepsilon_t^{\text{mid}} = \ln\frac{t_0}{t} \quad (3)$$

where $\varepsilon_t^{\text{mid}}$ is the thickness direction strain at the neutral surface and the variable t represents the actual sheet thickness at a certain wall angle.

When the strain condition of deformation is plane strain, the strain caused by pure bending can be calculated by Eq. (4) [3]:

$$\varepsilon_\Phi^A = \varepsilon_{\text{bending}} = \ln\frac{r}{R_m} \quad (4)$$

The actual thickness of sheet at the element location, which is an arbitrary small element in region A (shown in Fig. 1c), was set as t, and the radial distance from the tool center to the element was set as r. R_m represents the curvature of radius in the neutral surface of sheet. The median strain of the arbitrary element can be given by [3]

$$\varepsilon_\Phi^A = \varepsilon_{\text{bending}} + \varepsilon_{\text{stretching}} = \ln\frac{r}{R_m} + \ln\frac{t_0}{t} = \ln\frac{rt_0}{R_m t} \quad (5)$$

where $R_m = r_{tool} + (t/2)$ and it is noted that $R_m = r_{tool} + (t/2)$ works only for the bending condition of incremental forming in which the tool radius is significantly higher than the sheet thickness.

Regarding the strain state of the sheet in region A, the small element will be under tensile conditions, if an element satisfies $\frac{rt_0}{R_m t} > 1$. According to Eq. (5), the sheet material has maximum compression bending at the inner surface, which satisfies $r = r_{tool}$, and it can be obtained that the meridian strain will be zero, when the actual sheet thickness meets the condition where $t = t^* = -r_{tool} + \sqrt{r_{tool}{}^2 + 2r_{tool}t_0}$. The small element will be under compressive condition, when the actual sheet thickness meets $t > t^*$. Also, according to Eq. (6), there must be an area where the actual sheet thickness satisfies $t > t^*$ in the incremental forming

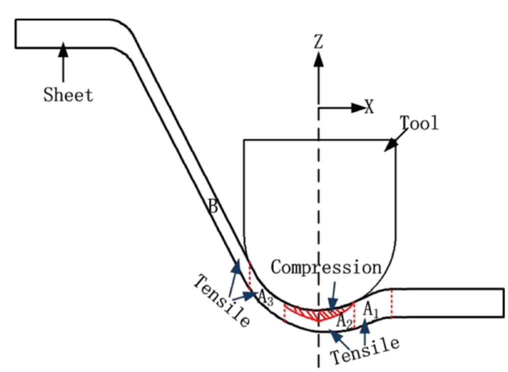

Fig. 6 A detailed tension-compression view

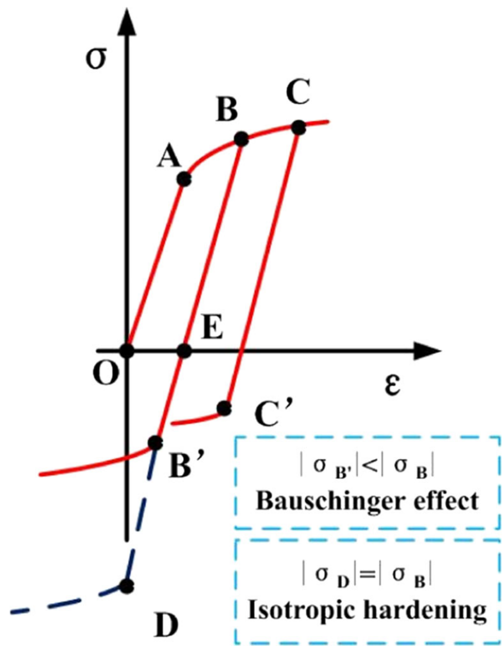

Fig. 7 Schematic representation of work hardening theory and the Bauschinger effect

process, as presented in Fig. 1c. Therefore, compressive area that is the result of the combined action of stretching and bending exists in the incremental forming process:

$$t_0 - t^* = t_0 + r_{tool} - \sqrt{{r_{tool}}^2 + 2r_{tool}t_0} > 0 \tag{6}$$

Figure 6 shows the tension and compression in each zone of incremental forming process. Due to the combined effects of bending and stretching, there is compression in the certain areas of the A_2 region. And, there is tension in the other deformation region. In the process, the deformation of A_1 region, the deformation of A_2 region, the deformation of A_3 region, and the deformation of B region are experienced successively. Thus, the zone near the interface of the sidewall experiences a tensile-compression-tensile cycle in the incremental forming process. The Bauschinger effect exists in the incremental forming process due to the existence of the complex loading path. It also produces softening so that the actual value is lower than the calculated value [15].

As presented in Fig. 7, deformation is extended until point B. Then, force is unloaded and the deformation reaches point E. Then, it was extended to the same direction again. Furthermore, it was considered that yield occurs when stress reaches the original stress associated with unloading. This comes as a result of work hardening [16].

The strain fields in Fig. 8a, b demonstrate the results of strain, indicating that the major strain contour and the minor strain contour of the part with a wall angle of 60° were formed by incremental forming. Each sidewall of the pyramidal parts is approximately in plane strain state, and the edge corner region is in a bi-axially oriented strain state. Additionally, the strain of sidewalls is evenly distributed for the parts with wall angles of 30°, 40°, 50°, and 60°. However, the strain distribution of the part with wall angle 20° is somewhat uneven in some region of the sidewall due to the orange peel effect. Thus, calculating the effective strain of each part requires statistical results, the average of effective strain of multiple points in the four sidewalls, for ensuring the accuracy of the calculation.

Six lines, located in the middle of the sidewalls, were selected for the strain measurement process (shown in Fig. 8c), and each line consists of 15 uniformly distributed points. The acquired data points were located in the region of tensile specimens of the pyramidal parts. Also, each data line was selected from the sidewall and was perpendicular to the rolling direction. The values of the first principal strain and the second principal, the thickness strain, strain of the acquired points can be obtained by ARGUS. The third principal strain can be obtained in accordance with the principle of constant volume of the plastic deformation, as given in Eq. (7).

$$\varepsilon_3 = -\varepsilon_1 - \varepsilon_2 \tag{7}$$

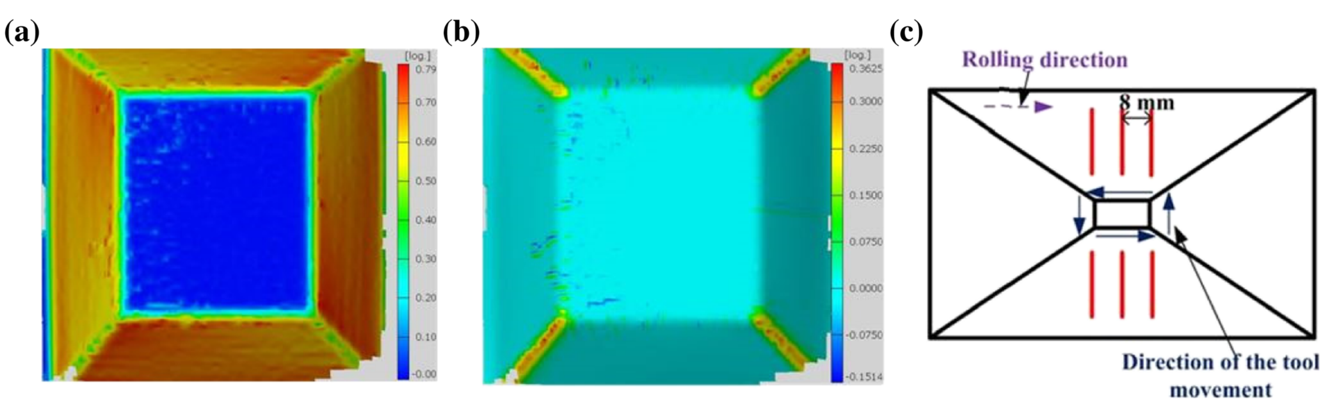

Fig. 8 True strain distribution of the pyramid with wall angle 60° (by ARGUS data measurement system). **a** The major strain. **b** The minor strain. **c** The acquired data point position

Table 1 The effective strain of each part formed by the incremental forming process

Wall angle	20°	30°	40°	50°	60°
Effective strain	0.0982	0.1602	0.3147	0.4883	0.7657

where ε_1 is the first principal strain, ε_2 is the second principal, and ε_3 is the third principal strain. And, the effective strain of each point is calculated by Eq. (8):

$$\overline{\varepsilon} = \frac{\sqrt{2}}{3}\sqrt{(\varepsilon_1 - \varepsilon_2)^2 + (\varepsilon_2 - \varepsilon_3)^2 + (\varepsilon_1 - \varepsilon_3)^2} \quad (8)$$

where $\overline{\varepsilon}$ is the effective strain. The average of effective strain of all acquired data points of each part was set as the corresponding effective strain, as presented in Table 1.

Each stress-strain curve after forming is shifted in accordance with the effective strain values presented in Table 1 along the strain axis in the curve of AA5754-O over the entire range of strain, as given in Fig. 9a. It shows that the true stress-strain curve of AA5754-O is located above the offsetting curves after forming. Also, the calculated yield strength, from the work hardening theory, can be obtained from the intersection of the extended true stress-strain curve of AA5754-O and the extension of linear elastic stage of offsetting curve, and the actual yield strength can be measured via tensile testing after incremental forming. Furthermore, Fig. 9b clearly shows that the calculated yield strength exceeds the actual yield strength of each wall angle. The calculated yield strength is obtained from the constitutive equation of AA5754-O and the effective strain. Thus, it can be obtained that softening occurs in the incremental forming process.

Figure 9b shows the difference between the calculated yield strength and the actual yield strength of each wall angle. This difference is caused by the Bauschinger effect. According to the Bauschinger effect, the actual yield strength is lower than the calculated value, when plastic deformation takes place in accordance with loading, unloading, and reverse loading [17, 18]. As presented in Fig. 7, the material is strained to point B, beyond yield point A, and then is unloaded. According to the work hardening theory, the tensile yield limit is increased from point A value, without plastic deformation, to point B value, when the material is strained again. However, the absolute value of tensile yield limit is decreased form the value of the point B to the value of point B′, if the material is loaded reversely after unloading, and the path OACC′ in Fig. 7 corresponds to a higher plastic deformation of the loading-unloading-reverse loading path.

It can be obtained that the difference between the actual value and the calculated value increases as the wall angle increases, as presented in Fig. 9b. Considering that the vertical feed of tool is a constant value, the transverse feed is lower in the case of the larger wall angle, and this insures that the total compressive area of large angle is higher than that of the small angle. Thus, the Bauschinger effect is more pronounced in the larger wall angle part.

Incremental forming is a process of complex stress. The accuracy of spring-back analysis depends on the prediction of stress level at the final stage of incremental forming, and also at the spring-back, which both are directly related to the Bauschinger effect of the material and cyclic hardening characteristics. The compressive zone and the Bauschinger effect in the research and production of incremental forming needs to be considered, such as spring-back prediction, spring-back compensation and establishing material model of simulation.

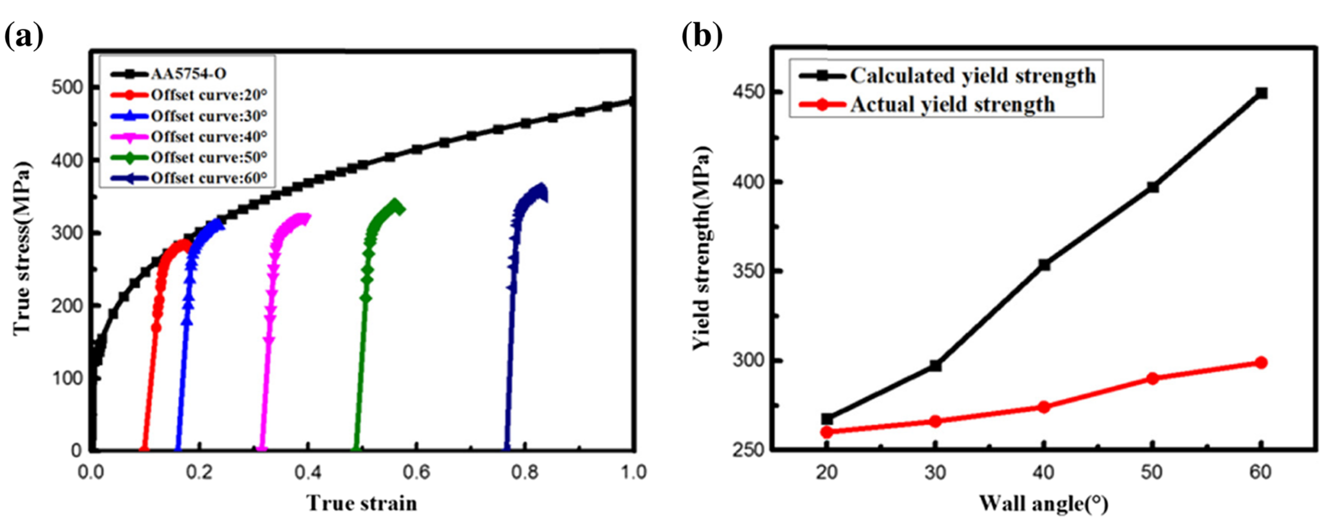

Fig. 9 The processing of offsetting curves. **a** Offsetting of the true stress-strain curve of each wall angle part. **b** Comparison of the calculated yield strength and actual yield strength

3.3 Mechanical properties of parts manufactured by incremental forming

The yield strength, ultimate tensile strength, and uniform elongation are usually used as mechanical properties index [19, 20]. Results present that the mechanical properties after deformation have changed considerably compared to the original state. The uniform elongation is decreased from 19.4% for the initial material to 6.1% for the 60° part, and the yield strength and ultimate tensile strength are increased from 124 and 290 MPa for the initial material to 299 and 361 MPa for the 60° part, respectively, as presented in Fig. 10. Meanwhile, it is also found that the uniform elongation decreases; the yield strength and ultimate tensile strength increases as the wall angle increases. This is because work hardening occurs in the parts formed with the incremental forming process. As dislocations grow, they increase and entangle each other when the sheet is formed by incremental forming under complex loading [21, 22]. There is a high volume of dislocation in the sidewalls of the pyramidal parts, due to the incremental forming process, and they obstruct the flow of defects which creates hardening effect when exerting forces are applied on the metal. And, the plastic deformation of the sheet becomes larger with the increase of wall angle, which result in strengthened work hardening [22]. It has been proved that the Bauschinger effect exists in the incremental forming process. However, compared to work hardening, the softening of the Bauschinger effect has little effect on the mechanical properties due to the Bauschinger effect occurring only in a small region which satisfies t > t*(as shown in Sect. 3.2). Therefore, work hardening plays a leading role in the change of mechanical properties.

The ultimate tensile strength value of 20° part is below the value of AA5754-O a little. One reason is the orange peel effect being present in the 20° part (shown in Fig. 2b). The orange peel effect, usually occurring in the incremental forming of small wall angle, is a kind of defect and can reduce the ultimate tensile strength. Furthermore, another reason may be that the Bauschinger effect offsets the work hardening in the 20° part. The work hardening may be not more pronounced than the Bauschinger effect in the 20° part under the circumstance of very small wall angle. Plus, the increase of the Bauschinger effect is less than the increase of the work hardening with increasing of wall angle.

The relation formulas between the mechanical properties and wall angle are obtained by fitting, as presented in Eqs. (9)–(11). It is also found that the fitting degree of the three formulas is quite high from Fig.11. These formulas can be used to predict the mechanical properties of the AA5754 parts manufactured by incremental forming in research and application. Meanwhile, the second derivatives of the formulas are obtained. From the second derivatives, it can be seen that the rate of decrease in uniform elongation and the rate of increase in ultimate tensile strength are decreasing at constant value with increasing of wall angle. The rate of increase in yield strength increases first and then decreases with increasing of wall angle.

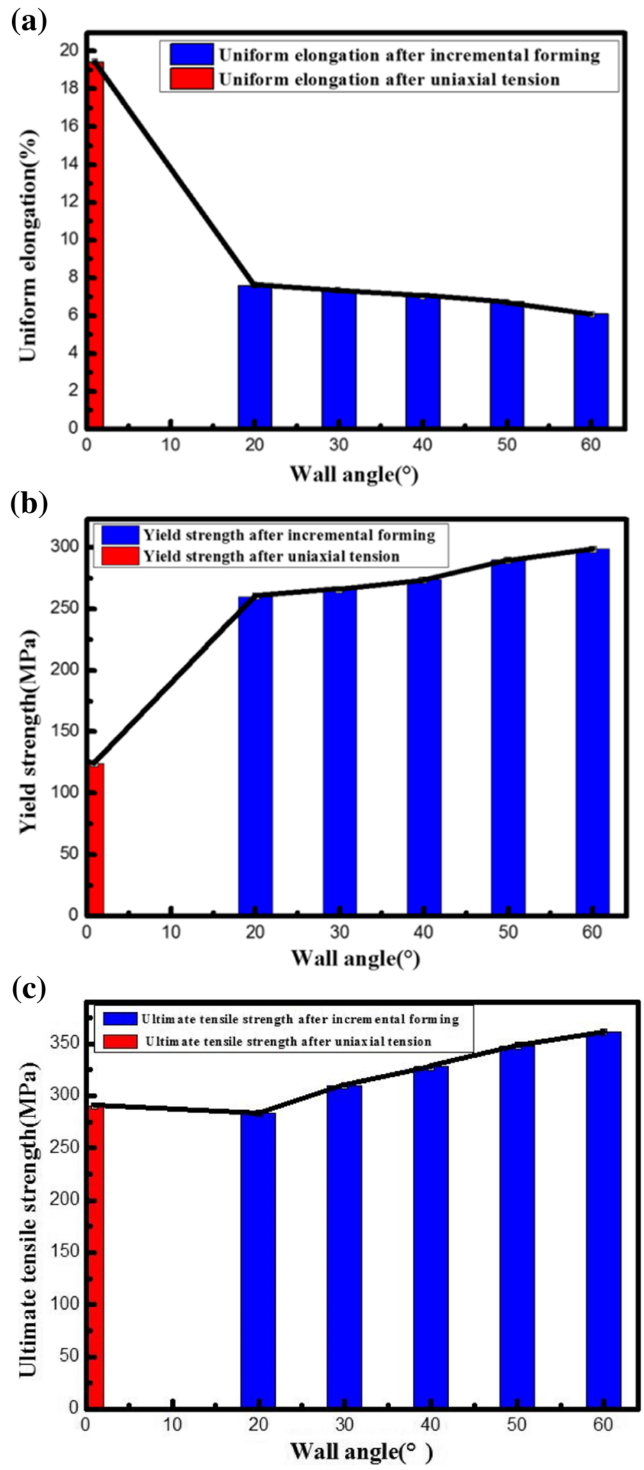

Fig. 10 The relation between mechanical properties and wall angle. **a** Uniform elongation. **b** Yield strength. **c** Ultimate tensile strength

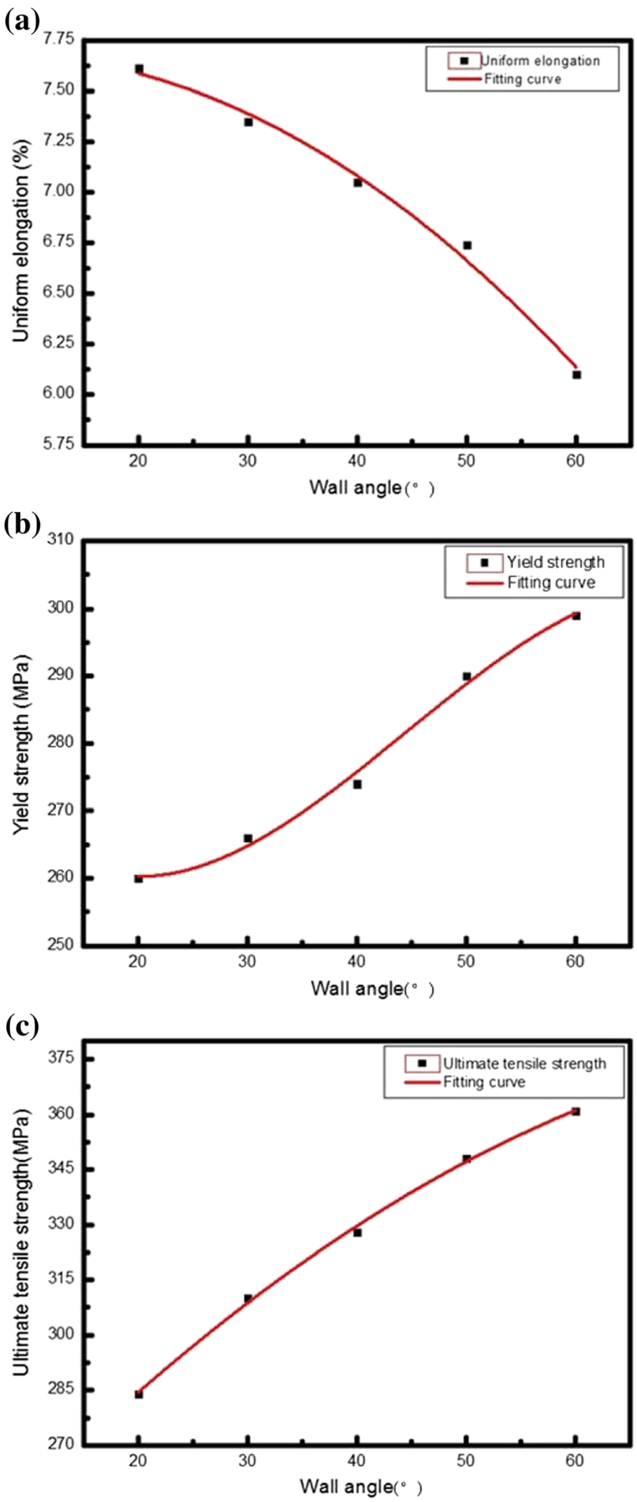

Fig. 11 The fitting of relation formulas between the mechanical properties and wall angle. **a** Fitting of uniform elongation. **b** Fitting of yield strength. **c** Fitting of ultimate tensile strength

The relation formula between the uniform elongation and wall angle:

$$\delta = 7.652 + 0.0077\alpha - 5.5 \times 10^{-4}\alpha^2 \quad (9)$$

The relation formula between the yield strength and wall angle:

$$\sigma_s = 288.8 - 3.125\alpha + 0.1\alpha^2 - 7.5 \times 10^{-4}\alpha^3 \quad (10)$$

The relation formula between the yield strength and wall angle:

$$\sigma_b = 225.4 + 3.29143\alpha - 0.01714\alpha^2 \quad (11)$$

where, α represents the wall angle of parts manufactured by incremental forming. δ, σ_s, and σ_b represent the uniform elongation, yield strength, and ultimate tensile strength of the parts.

4 Conclusions

This paper experimentally analyzed the influence of wall angle on the Bauschinger effect and mechanical properties in incremental forming process. A sheet of aluminum alloy AA5754-O was processed into pyramidal geometry of different wall angles for preparing tensile specimens. The tensile testing data of different wall angles was compared to each other and analyzed. The results of the current research can be summarized as follows:

There is a compressive area around the tool center, and the complex loading causes the existence of the Bauschinger effect in the incremental forming process of AA5754. Also, the influence of Bauschinger effect increases with the increasing of wall angle.

The incremental forming parts have very small uniform elongation and large yield strength. The uniform elongation decreases, and the yield strength and ultimate tensile strength increases as the wall angle increases. And, the formulas for predicting the mechanical properties at different wall angles are obtained.

The Bauschinger effect and the work hardening occur simultaneously in the incremental forming process of AA5754. And, the work hardening plays a leading role in the change of mechanical properties.

Acknowledgements The authors would like to thank the Fundamental Research Funds for the Central Universities (grant number NS2016052).

References

1. Centeno G, Bagudanch I, Martínez-Donaire AJ, García-Romeu ML, Vallellano C (2014) Critical analysis of necking and fracture limit strains and forming forces in single-point incremental forming. Mater Des 63(21):20–29
2. Martins PAF, Bay N, Skjoedt M, Silva MB (2008) Theory of single point incremental forming. CIRP Annals - Manuf Technol 57(1): 247–252

3. Fang Y, Lu B, Chen J, Xu DK, Ou H (2014) Analytical and experimental investigations on deformation mechanism and fracture behavior in single point incremental forming. J Mater Process Technol 214(8):1503–1515
4. Silva MB, Skjoedt M, Atkins AG, Bay N, Martins PAF (2008) Single-point incremental forming and formability–failure diagrams. J Strain Anal Eng Des 43(1):15–35
5. Allwood JM, Shouler DR, Tekkaya AE (2007) The increased forming limits of incremental sheet forming processes. Key Eng Mater 344:621–628
6. Shrivastava P, Tandon P (2015) Investigation of the effect of grain size on forming forces in single point incremental sheet forming. Procedia Manufacturing 2:41–45
7. Shanmuganatan SP, Kumar VSS (2014) Modeling of incremental forming process parameters of al 3003 (O) by response surface methodology. Procedia Engineering 97:346–356
8. Gatea S, Ou H, Mccartney G (2016) Review on the influence of process parameters in incremental sheet forming. Int J Adv Manuf Technol 87:479–499
9. Vol N (2003) Effect of wall angle on Al 3003 strain hardening for parts formed by computer numerical control incremental forming. Proc Inst Mech Eng 217(11):1571–1579
10. Jin K, Guo XZ, Tao J, Wang H, Kim N, Gu YB (2016) A model of one-surface cyclic plasticity with Lemaitre damage criterion for plastic instability prediction in the incremental forming process. Int J Mech Sci 114:88–97
11. Jun-Chao LI, Chong LI, Zhou TG (2012) Thickness distribution and mechanical property of sheet metal incremental forming based on numerical simulation. Trans Nonferrous Metals Soc China 22(10):s54–s60
12. Amouzegar H, Schafer BW, Tootkaboni M (2016) An incremental numerical method for calculation of residual stresses and strains in cold-formed steel members. Thin-Walled Struct 106:61–74
13. Hadoush A, Boogaard AHVD, Emmens WC (2011) A numerical investigation of the continuous bending under tension test. J Mater Process Technol 211(12):1948–1956
14. Ai S, Lu B, Chen J, Long H, Ou H (2017) Evaluation of deformation stability and fracture mechanism in incremental sheet forming. Int J Mech Sci 124-125:174
15. Dell HD, Eliseev VV, Shapievskaya VA (2014) Experimental study of the Bauschinger effect for anisotropic metals. Mech Solids 49(5): 561–567
16. Balík J, Dobroň P, Chmelík F, Kužel R, Drozdenko D, Bohlen J (2015) Modeling of the work hardening in magnesium alloy sheets. Int J Plast 76:166–185
17. Paul JDH, Hoppe R, Appel F (2016) On the Bauschinger effect in TiAl alloys. Ac Mate 104:101–108
18. Kafka V, Vokoun D (2013) Causality in the Bauschinger effect generation and in other deformation processes in metals. Eur J Mech - A/Solids 42(6):395–401
19. Cao Z, Wang F, Wan Q, Zhang Z, Jin L, Dong J (2015) Microstructure and mechanical properties of AZ80 magnesium alloy tube fabricated by hot flow forming. Mater Des 67:64–71
20. Zhang X, Huang T, Yang W, Xiao R, Liu Z, Li L (2016) Microstructure and mechanical properties of laser beam-welded AA2060 Al-Li alloy. J Mater Process Technol 237: 301–308
21. Narayanasamy R, Anandakrishnan V, Pandey KS (2008) Effect of geometric work-hardening and matrix work-hardening on new constitutive relationship for aluminium–alumina P/M composite during cold upsetting. Int J Mech Mater Des 4(3):301–315
22. Yi HY, Yan FK, Tao NR, Lu K (2016) Work hardening behavior of nanotwinned austenitic grains in a metastable austenitic stainless steel. Scr Mater 114:133–136